

SEMI-ANNUAL STATUS REPORT  
NASA Grant SC-NGR 44-012-055

to

The University of Texas at Austin

for the period

May 1, 1967 to October 31, 1967

I. Introduction

The present grant supports the continued study of polarization and time structure of Jupiter's decametric radiation. Progress will be summarized in two sections:

- fabrication and installation of instrumentation at the University of Texas Radio Astronomy Observatory and at spaced receiver sites.
- development of analysis program for use in reduction of data from the GSFC synoptic monitoring network.

II. Instrumentation

1. Main Observing Site

A number of radio telescope systems have become operational during the current report period: the meter wavelength interferometer for discrete source studies, and 10, 16, 20, 22 and 30 MHz interferometer for synoptic monitoring of Jupiter.

The 16.7 and 22.2 MHz polarization antennas were completed and have been tested and are ready for use.

An interim-slow-speed paper tape digitizer system is being used for data recording pending the completion of the high-speed magnetic tape data acquisition system.

Two observers are trained and managing the equipment during the 10 hours daily Jupiter observing period.

2. Spaced Receivers Site

Final completion of formalities required for use of the spaced receiver sites occurred on February 1, 1968; orders for power, telephone and fencing have gone out, and equipment installation will begin in about one month.

### 3. Microwave Link

Licenses for operation of the microwave links were finally received in July, 1967. This permitted final tune up of transmitters, receivers and antennas for the assigned frequencies to begin. Testing of the entire link system at the Radio Astronomy Lab in Austin was completed in November, 1967. Currently, the terminal station at the main site and the Mt. Ord relay station are in place. The spaced site terminals are ready for installation once the preliminary site development is complete and power is available.

### 4. Receiver System

A number of problems with the Yale polarimeters were discovered during analysis described in the last progress report, which necessitated substantial re-design of parts of the receivers and particularly of the calibration systems. The problems have been solved, and the receiver systems will be ready before spaced receiver site development is complete. In particular, the main site four-component dual frequency polarization analyzers will be operational in mid-February.

### 5. High Speed Data Acquisition System.

The high speed data acquisition system is the major equipment item provided by the present grant; major component parts were purchased and arrived during September and October; assembly of the system is still in progress at the Radio Astronomy Laboratory. The resulting data acquisition system will have great speed and flexibility and will permit very rapid analysis of the data obtained when the microwave links become operational.

## III. Data Analysis

### 1. Time Structure Data

Considerable progress in analysis of the backlog of analog data obtained at Yale was made during the report period; nearly all the records that repay the labor have now been done. The attached Internal Report (#10 by Louis P. Pataki) summarizes this phase of the work.

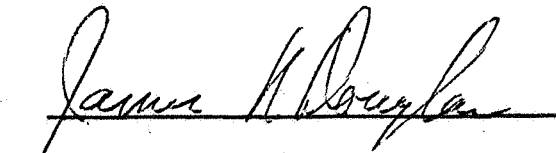
### 2. Synoptic Monitoring Data

J. N. Douglas and F. A. Boyzan completed the analysis of the backlog of monitoring speed data, and Mrs. J. Pataki has brought the data catalog up to date. This catalog now contains occurrence information for the period 1950 - 1966, and analysis procedures are now underway.

### 3. Programming.

F. A. Bozyan and J. W. Lindsey completed a number of computer routines which will be used with the Goddard data tapes. Of particular interest is a program which automatically identify Jupiter storms, and a program which

super-synthesizes a larger aperture for calibration of antenna gains using discrete radio sources.



James N. Douglas  
Principal Investigator  
16 February 1968

JND:jm

The University of Texas  
Radio Astronomy Observatory

Internal Report #10

February 9, 1968

Spaced Receiver Observations of Jovian Decameter Flux  
[Status of Reduction]

Louis P. Pataki

The second long "L" pulses in Jupiter's decameter radio emission are caused by interplanetary propagation effects. Elements of the solar wind act as a screen which creates phase changes in the emissions passing through it. These changes create interference patterns which build into patterns of amplitude fluctuation. We observe these fluctuations as "L" pulses. Large scale systematic motion in the solar wind is reflected on Earth as a drift in the pattern of amplitude fluctuation across the observing plane. Correlation studies of this amplitude pattern give us a set of correlation contours which reflect the nature and motion of the interplanetary medium as well as the intricacies of the source of the radiation.

Among the collection of Jupiter's events recorded with the 22.20 Mc spaced receiver equipment at the Yale Observatory and its remote stations which have been digitized at Yale and the University of Texas, three, those of 23 and 26 October 1965 and that of 14 December 1965, have proven useful for a full, three station, analysis. Recent emphasis in data reduction has fallen on the records of these events although the collection of events recorded satisfactorily at one or two station contains a far more extensive set of observations and contain, in some cases, very interesting effects in their own right.

Internal report 3 (See reference list) considered the analysis of lags in the reception of amplitude peaks at widely spaced stations. Report 4 considered the determination of the characteristic ellipse of contours of equal amplitude correlation on an observing plane. Report 5 considered refinements in the treatment necessary for an unbiased correction for noise effects. The set of digitized two station records has been processed in a consistent manner and cor-

relation results for these events are presented. Various data reduction techniques which have been developed are described.

Records of 25 events, two recorded at four stations, three at three stations and 21 at two stations have been put through the correlation routines. The correlation graphs resulting from this processing are given as appendix I. Table I summarizes 40 records of 20 events. It does not include the 1961 records or the 17NOV64 or 30 January 1965 events.

In an attempt to find some order in this data, the events were sorted by peak crosscorrelation coefficient. The logic for this is as follows. If the phase changing screen responsible for the amplitude scintillations (i.e. the interplanetary medium) is drifting along the line between the observing stations and if the structure of the medium itself is stationary in a statistical sense, then the peak crosscorrelation coefficient is a measure of the quality of the records being correlated. Except near Jovian opposition, the stations lie very close to the projection of the ecliptic on the observing plane (Douglas and Smith, 1967) and this is thus a reasonable sorting scheme. Table II shows the results of this sorting.

TABLE I

## CHARACTERISTICS OF THE CORRELATION GRAPHS 1964-1965

Halfwidths of Autocorrelation Graph to  $\rho = 0.50$ 

Number of Correlations	14	14	10	1	1
Halfwidth (Seconds)	$\tau \leq 0.5$	$0.5 < \tau \leq 1.0$	$1.0 < \tau \leq 1.5$	$1.5 < \tau \leq 2.0$	$2.0 < \tau$

Shape of Autocorrelation Graph

Number of Correlations	18	6	14	2
Description	Simple Shape Dropping To $\rho < 0.20$ in 3 sec.	Simple Shape Dropping To $\rho < 0.20$ in 3 sec.	More Than One Maximum	Other

Peak Value of Crosscorrelation

Number of Events	2	4	2	3
$\rho$ Max.	$0 < \rho \leq 0.1$	$0.1 < \rho \leq 0.2$	$0.2 < \rho \leq 0.3$	$0.3 < \rho \leq 0.4$
Number of Events	2	1	2	1
$\rho$ Max.	$0.4 < \rho \leq 0.5$	$0.5 < \rho \leq 0.6$	$0.6 < \rho \leq 0.7$	$0.8 < \rho \leq 0.9$

## KEY TO TABLE II

### Crosscorrelation Type Identification:

- I            sharp, clearly defined maximum.  $n - .1 < \rho_{\max} \leq n$   
II           broad maximum.  $n - .1 < \rho_{\max} \leq n$   
III          no clearly defined maximum.

### Autocorrelation Type Identification:

- I            drops gradually to a value  $\rho < 0.3$  in lag  $< 3S_0$   
Ia           drops rapidly to a value  $\rho < 0.3$  in lag  $< 3S_0$   
II           drops gradually to a value  $\rho < 0.3$  in lag  $< 3S_0$  and has secondary peak  
IIa          drops rapidly to a value  $\rho < 0.3$  in lag  $< 3S_0$  and has secondary peak  
III          drops to a value  $\rho < 0.3$  in  $\tau > 3S_0$

This terminology was adopted for convenience in describing the correlation graphs. It is fully defined by this key and is not meant to have any other significance. For examples compare items in Table II with figures in Appendix I.



TABLE II

Date	Indices	Crocor Type	Autocor BSR Type	Autocor BSR Width	Autocor PSR Type	Autocor PSR Width
29 Jan 65	1916	I.1	II-III	$1.0 < \tau < 1.5$	II-III	$1.0 < \tau < 1.5$
31 Jan 65	900	II.1	III	$3.0 < \tau$	IIa	$\tau < .25$
13 Feb 65	1100	I.2	I-II	$\tau \sim .5$	I-II	$\tau < .5$
31 Jan 65	1212	II.2	I	$.5 < \tau < 1.0$	Ia	$\tau < .25$
25 Jan 65	968	II.2	II	$.5 < \tau < 1.0$	IIa	$\tau < .25$
12 Jun 64	1200	I.2	IIa	$\tau < .25$	IIa	$\tau < .25$
30 Sep 64	236	II.3	II	$.5 < \tau < 1.0$	IIa	$\tau < .25$
23 Jun 64	935	I.3	I	$\tau < .5$	I-Ia	$\tau < .25$
20 Jan 65	1056	I.4	III	$1.0 < \tau < 1.5$	I-Ia	$\tau < .25$
30 Sep 65	614	I.4	I-II	$1.0 < \tau < 1.5$	I-II	$\tau < .5$
12 Jun 64	734	I.4	IIa	$\tau < .25$	IIa	$\tau < .25$
05 May 64	725	I.5	III	$\tau \sim 1.0$	I-II	$\tau < .5$
05 May 64	701	I.5	II	$\tau < .5$	I-II	$\tau < .5$
04 Feb 65	1068	I.6	II-IIa	$\tau < .25$	II-IIa	$\tau < .25$
10 Jan 65	852	I.7	I-II	$\tau \sim 1.0$	I-II	$.5 < \tau < 1.0$
27 Jan 65	584	I.8	I	$.5 < \tau < 1.0$	I	$.5 < \tau < 1.0$
10 Jan 65	664	I.8	I	$\tau \sim 1.0$	I	$1.0 < \tau < 1.5$
26 Dec 64	598	I.8*	II	$.5 < \tau < 1.0$	I	$.5 < \tau < 1.0$
						2228 EST
						2009 EST
						1100 EST
						1053 EST
						1805 EST
						1816 EST

TABLE II (Continued)

Date	Indices	Crocor Type	Autocor BSR		Autocor PSR	
			Type	Width	Type	Width
30 Sep 64	224	II.8	I	$1.0 < \tau < 1.5$	III	$1.0 < \tau < 1.5$
20 Jan 65	352	I.9	II	$1.0 < \tau < 1.5$	II	$1.5 < \tau < 2.0$
18 Jul 61		I.9*	II	$0.5 < \tau < 1.0$	II	$0.5 < \tau < 1.0$
						Complex structure
						Digitized each 1/10 sec.

\* Plus enhanced correlation at lag  $\tau = 0$

Listing the records in a form such as Table II is very revealing. Recall that the table was constructed without consideration of the autocorrelation graphs. These, however, have fallen into a pattern. The lower peak correlation values are associated with the fast drop off "a" records and with the broad III records. The former are seen (by inspection of the records themselves) to be associated with records with poor signal to noise ratio - either because of a large noise term (for which correction can be made) or because Jupiter is in evidence only a small fraction of the time. This was checked by subdividing one of the long records. The autocorrelation I have labeled Type III is evidently representative of a large low frequency component in the record (e.g. baseline shift). A digital program has been devised to filter the data. The program takes the form of a convolution - equivalent to a multiplicative filter in the fourier transfer domain. When it is used on time series records, it is, in its effect, a frequency filter. As the shape of the filter is a controllable variable, the routine is particularly valuable in assessing the utility of various filter schemes. Work is in progress to see if the autocorrelation labeled III can be improved by a suitable filtering process and whether various interesting sections of the frequency spectrum can be isolated by these techniques for further analysis.

The two events noted as having a high correlation at zero lag (higher than would be expected by interpolation) were both records rich in "S" pulse structure. As these have been found to show no measurable lag on our time scales (Perry 1966), the enhanced correlation at zero lag is a reflection of the correlation of these pulses.

The two stations record of 29 January 1965 which was reduced for 1352 consecutive quarter seconds was subdivided into three separate records of about 2 minutes each and again reduced to correlations. Thus these resulting sets of graphs indicate the effects of different sources of noise in the records. The segment beginning at 1916EST is characterized (these comments reflect a visual description of the records) by much uncorrelated signal. Extremely strong signals occurring in the Pomfret record are not seen in the Bethany record. These signals are most probably local interference. The pulses appearing on both records and having the typical shape of the Jupiter event are much weaker than the interference burst and occur infrequently.

The segment beginning at 1918EST again has a low occurrence rate of Jovian emission and the beginning section has some intense short amplitude spikes in the Bethany channel which cannot be found in the Pomfret record.

The segment beginning at 1920EST can only be described as an excellent record. The signal to noise ratio is good in both channels and Jupiter pulses are very much in evidence. There appear to be two time structures one of the order one second and a longer one of some few second and a longer one of some few seconds.

The correlation graphs of this record reflect these effects. The six minute data, reflecting the low average occurrence of Jupiter radiation shows a rather low crosscorrelation. The graphs of the data from 1916 reflect the presence of a large amount of uncorrelated noise. The records from 1918 again reflect the infrequent occurrence in this section while the graph of the data from 1920 reflect the excellence of this

section of record..

It is of interest, however, to note that no matter which record was used, one would draw the same conclusion about the lag to peak correlation. The relatively broader peak in the 1920EST graph may reflect the presence of the longer pulses noted in this section of the record. Even the extremely poor record of 1916-1918EST gives a lag to peak correlation consistent with the better parts of the record.

The presence of radiation pulses of varying widths and of low frequency noise (e.g. gradual baseline shifts) indicates that there may be a promising direction of study available through analysis of the data after various filter operations as outlined above.

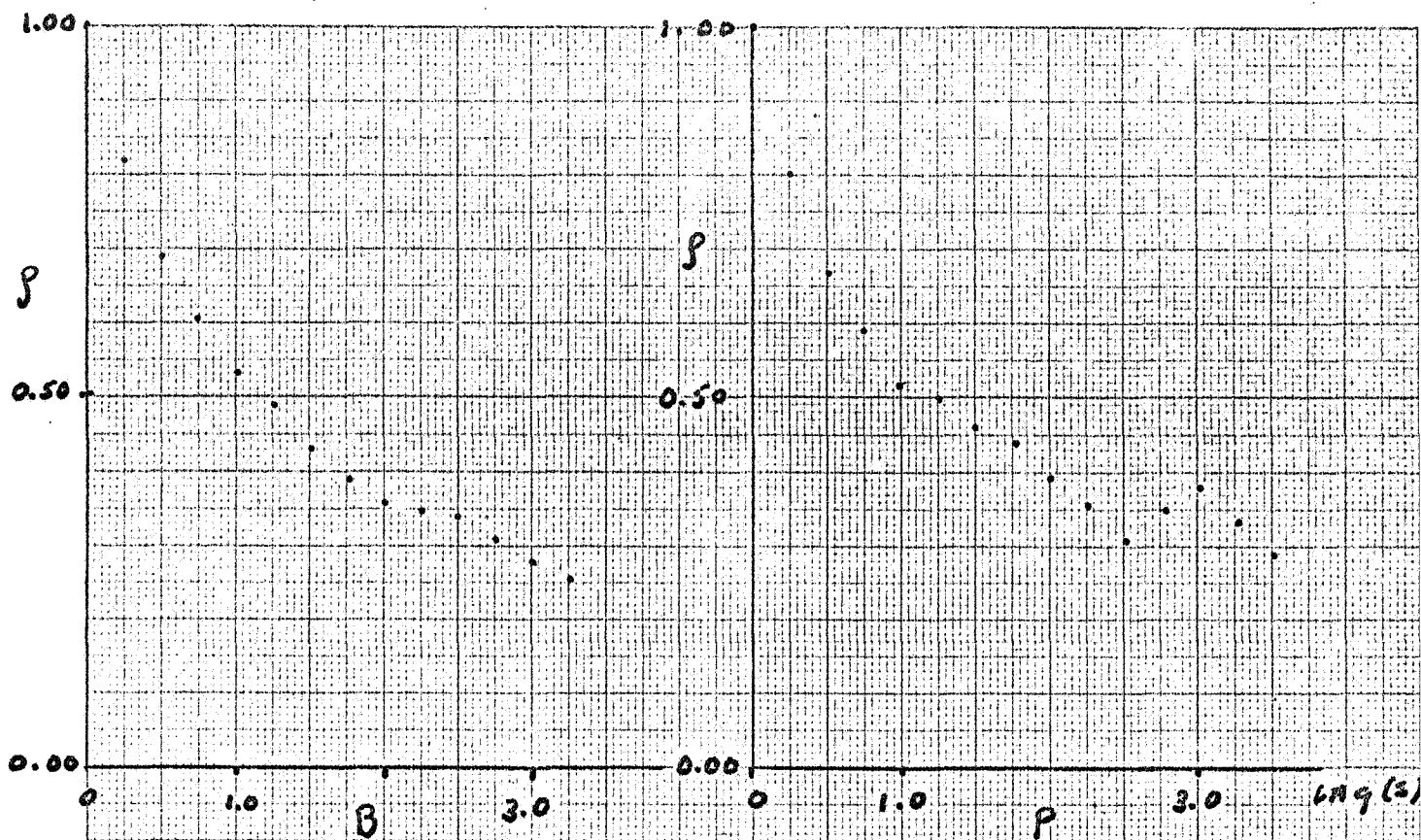
### Key to Figure 1

The graphs on the next four pages refer to the observations on 29 January 1965. The first set of graphs represents all the data while the next three are subdivisions as described in the text. The labels B, P, B-P refer to receivers at the Bethany observing station, Bethany, Connecticut and the spaced station at Pomfret, Connecticut. The crosscorrelation is in the sense of Bethany leading Pomfret.

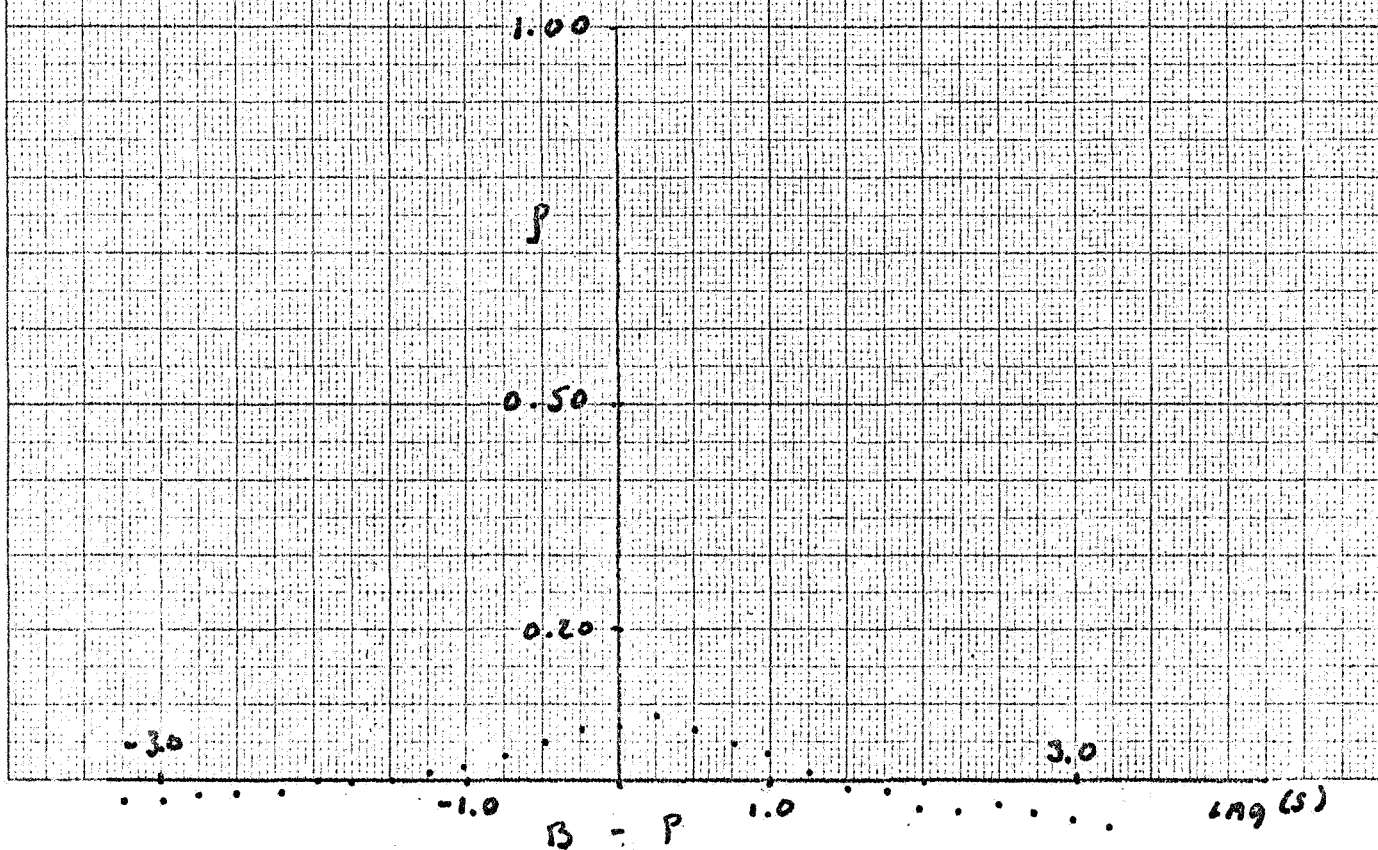
29 JAN 65 1916 EST 1352 INDICES

EUBENE DIETZEN CO.  
MADE IN U. S. A.

NO. 340-M DIETZEN GRAPH PAPER  
MILLIMETER



AUTO CORRELATION

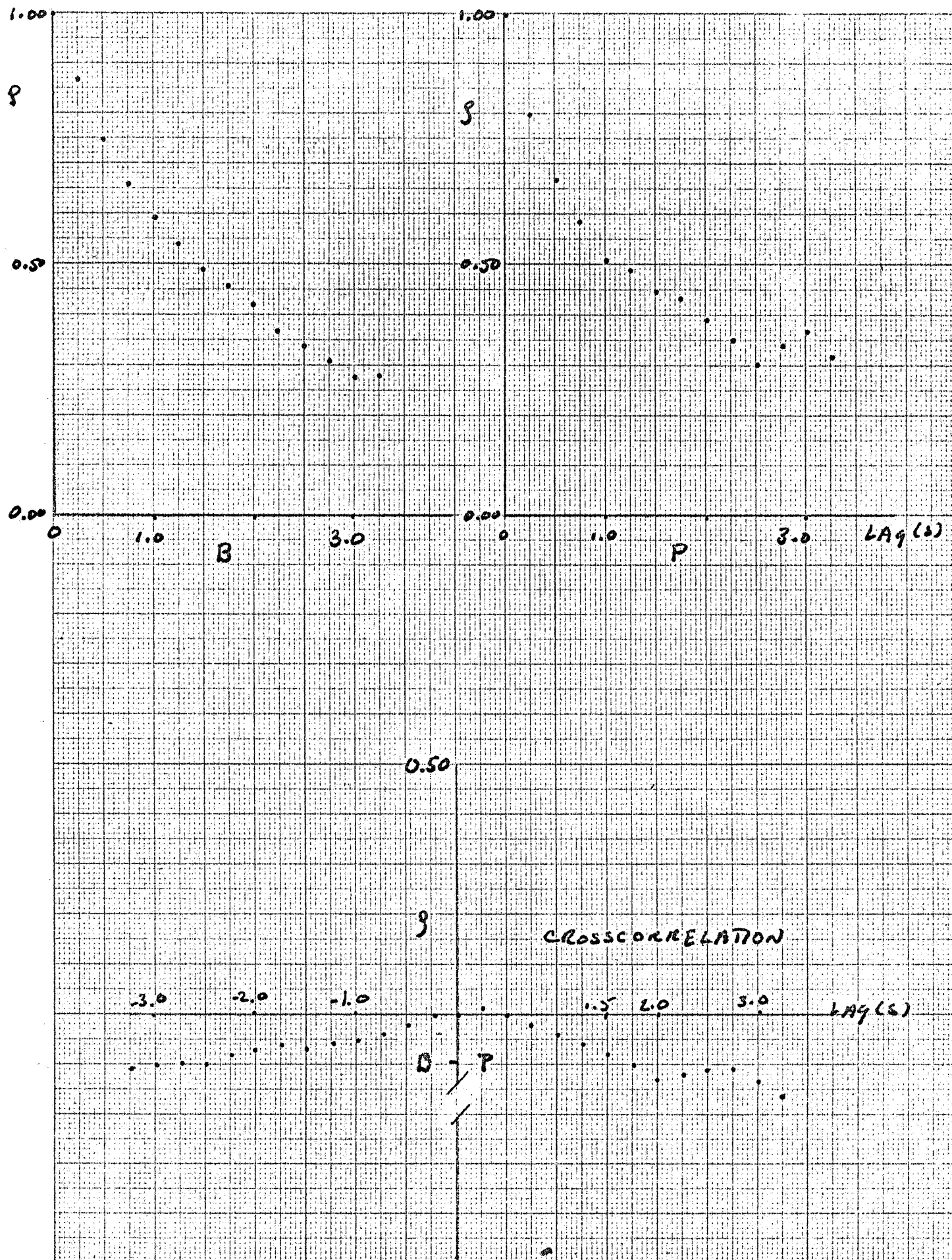


CROSS CORRELATION

29 JAN 65 1916 EST 462 INDICES

EUGENE DIETZEN CO.  
MADE IN U. S. A.

NO. 340-M DIETZEN GRAPH PAPER  
MILLIMETER

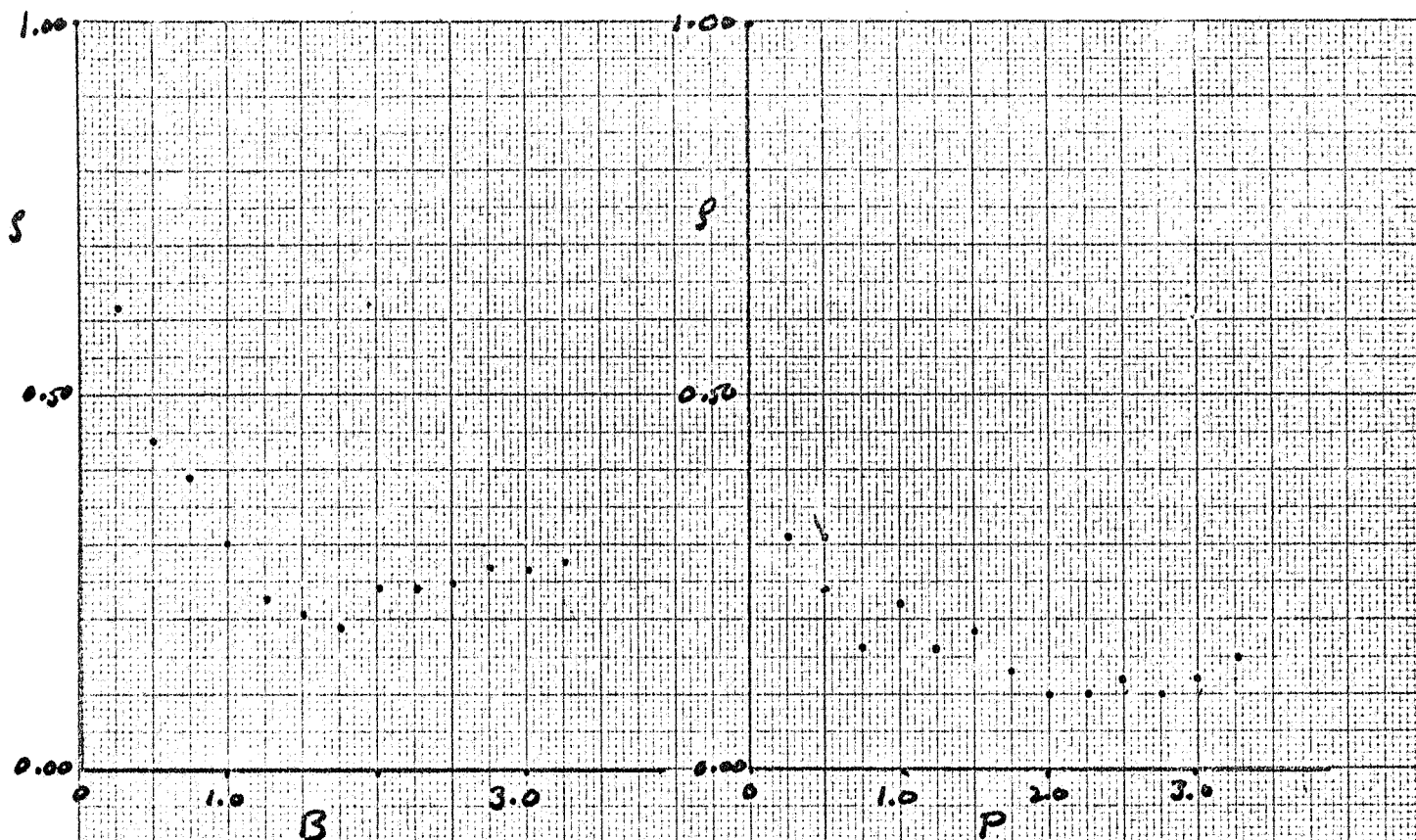




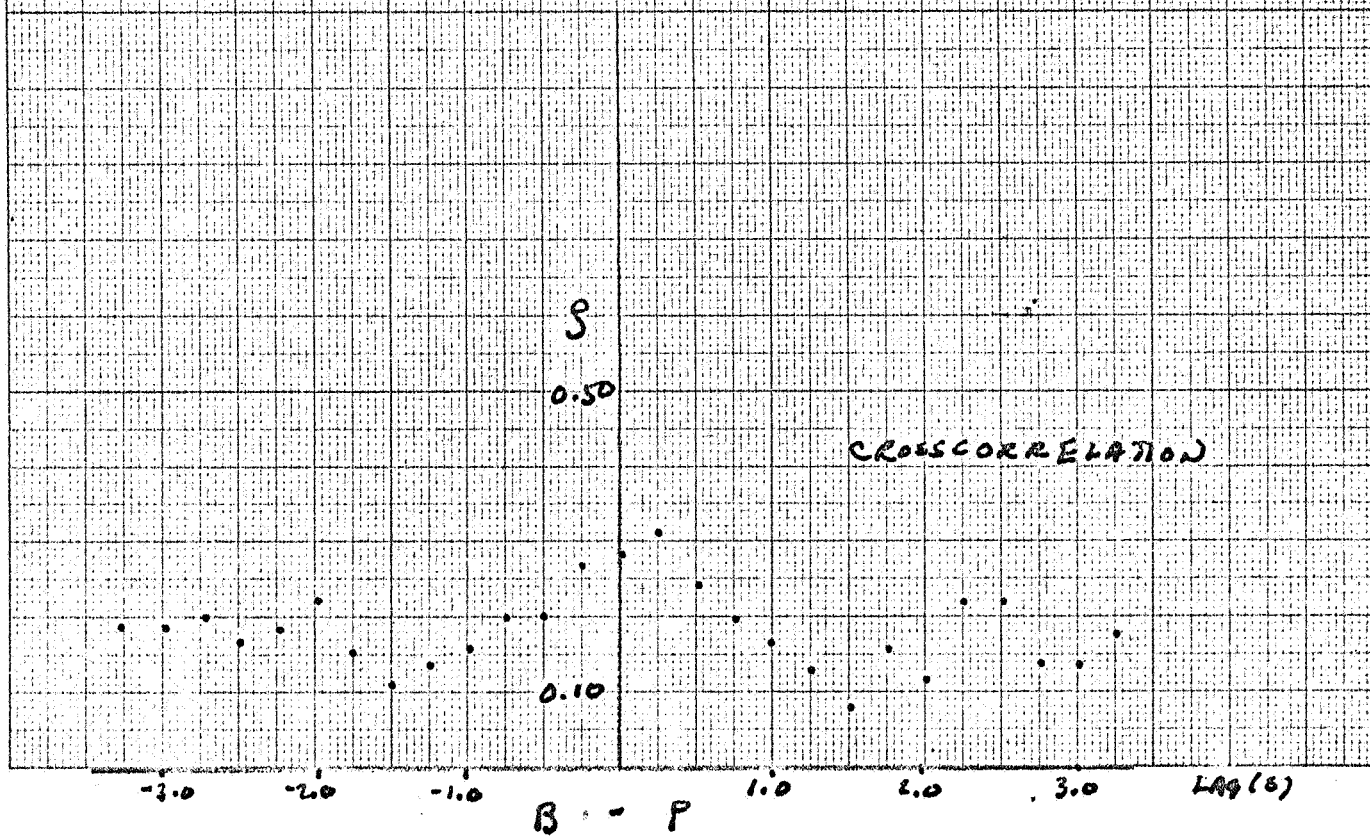
29 JAN 65 1918 EST 462 INDICES

EUGENE DIETZEN CO.  
MADE IN U. S. A.

NO. 340-M DIETZEN GRAPH PAPER  
MILLIMETER



AUTOCORRELATION

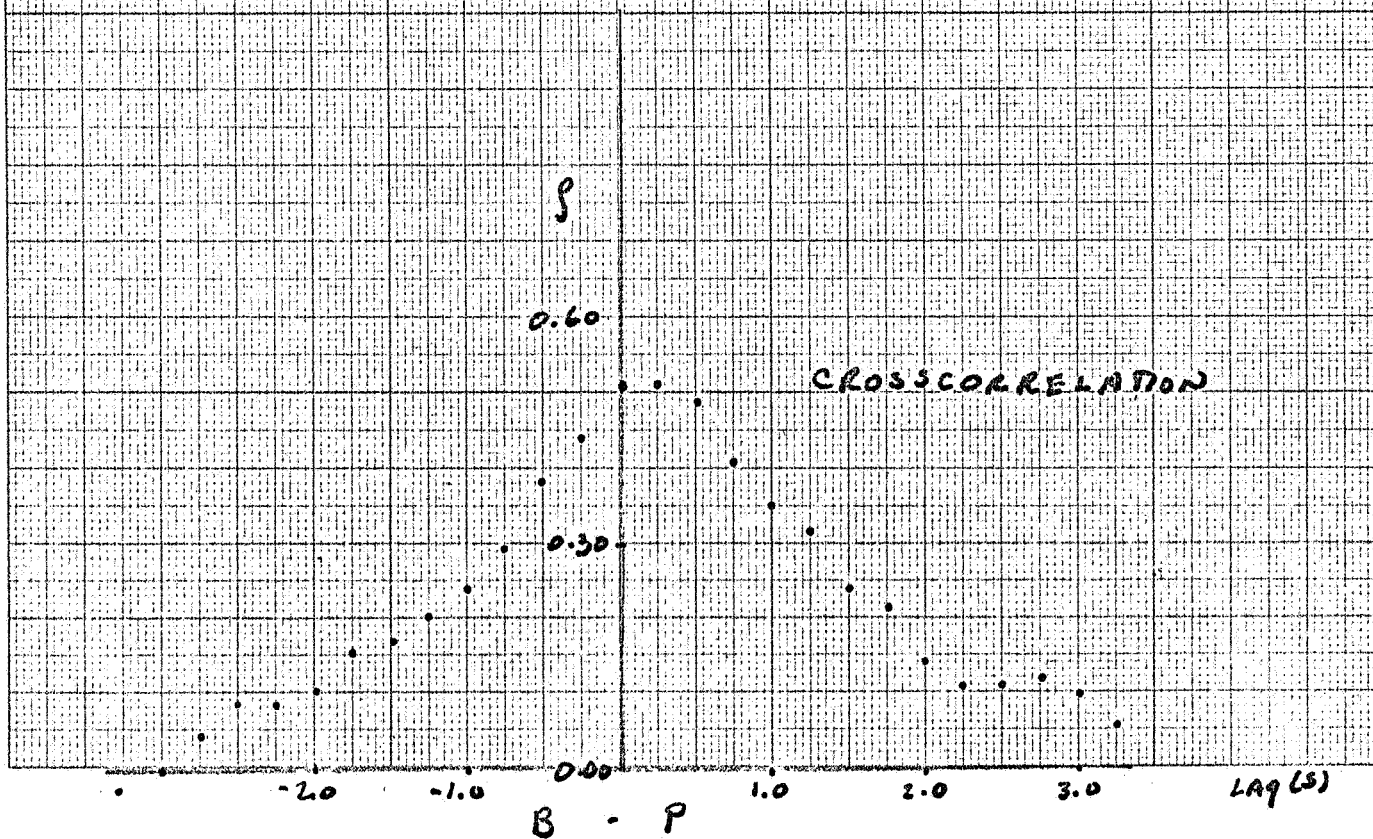
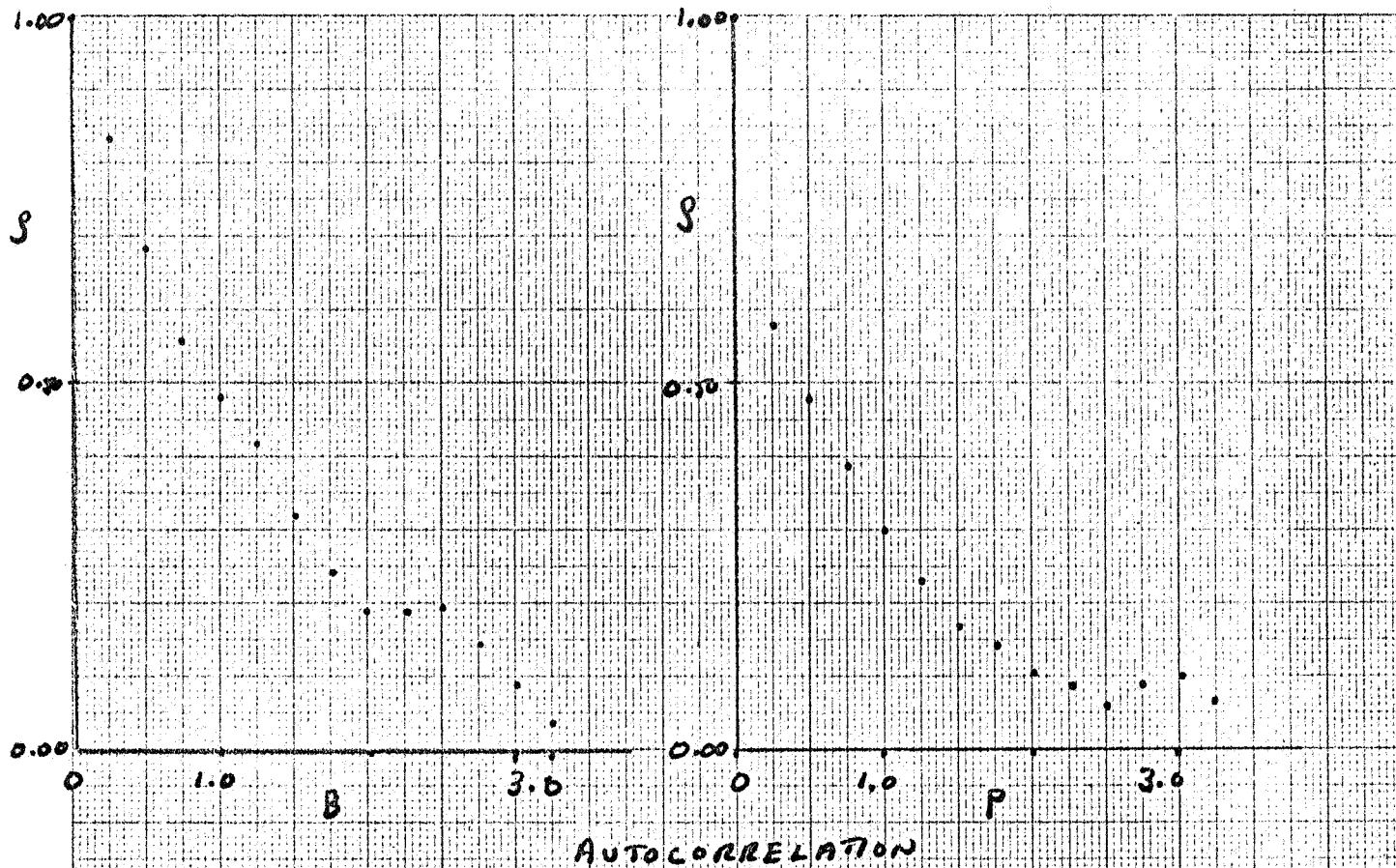


CROSSCORRELATION

29 JAN 65 1920 EST 428 INDICES

EUGENE DIETZEN CO.  
MADE IN U. S. A.

NO. 340-M DIETZEN GRAPH PAPER  
MILLIMETER



The three station analysis has continued. As we found the lag data to be relatively insensitive to noise effects in the records (see analysis of noise effect in Internal Report 5 and discussion of detailed analysis of a two station record above), it seemed worthwhile to carry out as much analysis as was possible using lag techniques. If the contours of equal correlation are circular, one can obtain a solution for the velocity of the phase changing screen causing correlated amplitude scintillations from the observed lags alone. While a 90% confidence level error bar on correlation derived parameters includes the circular contour solution, this solution is not the best fit to the data. Nevertheless, this analysis is so insensitive to many of the possible sources of error such as ionospheric scintillation and differential noise effects or Faraday rotation between station - all of which may effect the numerical values of correlation (not needed for the circular analysis), that it is a valuable approximation to the correct solution.

Figure 2 shows the situation for the observations of 23 October 1965. We are to fit an ellipse through three points,  $(r_i, \theta_i)$ . In each case  $\theta_i$ , being constrained by the geometry of the observing program, is exactly known. There is an error in  $r_i$  which arises from noise in the observations and from statistical error in the values of crosscorrelation which were used in its calculation. In each case, the most probably value is denoted by o while the extremes to the 90% confidence level in the statistical validity of the correlation coefficient (neglecting system noise) are denoted by x. It is seen that the circular solution is within these limits.

If we divide the distance between two stations by the time lag

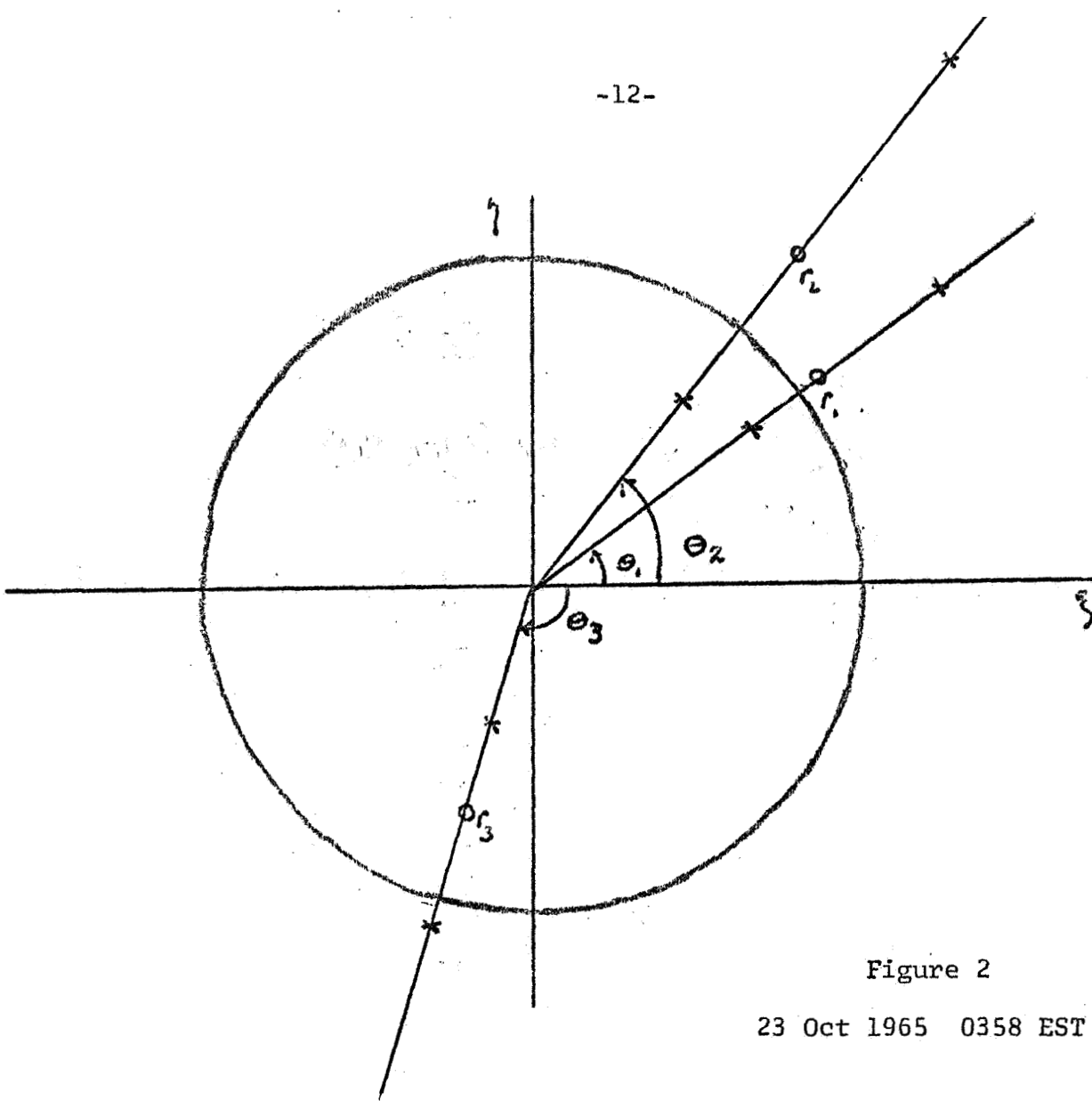


Figure 2

23 Oct 1965 0358 EST

Points of equal correlation in velocity coordinates

Circle illustrates possible circular fit to the three points

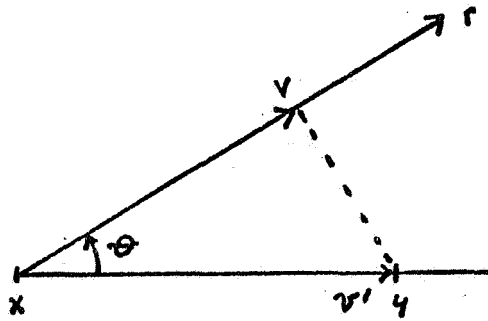
(see text)

necessary for peak crosscorrelation of amplitude at these stations, we have what may be called, by analogy to the ionospheric case, the "fading velocity" in the direction of one station from the other. This velocity is the velocity the phase changing screen causing the amplitude fluctuations would have if it were moving along that line. In general, of course, it is not. A combination of two pairs of such observations uniquely gives the true velocity as it is reflected upon the observing plane. With three stations we have three pairs of stations and a redundant answer. From a theoretical view it becomes obvious that it is entirely redundant. Thus, given three sets of amplitude data we should get an exactly redundant answer. The extent to which we do is a measure of the accuracy of the analysis of the data. Numerical noise in the correlation or the calculations and errors in estimate of lag will show up here. Reflection on the method, however, reveals that the coincidence of the answers gives no check on the accuracy of the initial assumptions. Figures 3 and 4 make the procedure clear.

FIGURE 3

Correlation Drops at an Equal Rate in all Directions  
(Circular Correlation Contours)

Two Station Observations



If the projected velocity of the screen causing the fluctuations is along  $r$ , the peak crosscorrelation between amplitude observations at  $x$  and  $y$  occurs with delay  $t$  such that

$$t \text{ [sec]} = (y-x) \text{ [km.]} / v' \text{ [km./s.]}$$

note  $v' = v/\cos \theta$ . Thus  $t$  is smallest (zero) when the velocity is perpendicular to the line between stations.

FIGURE 4

Correlation Drops at an Equal Rate in all Directions  
(Circular Correlation Contours)

Three Station Observations

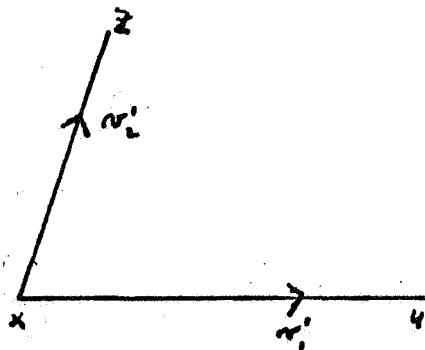


Figure 4 a) observed apparent velocities

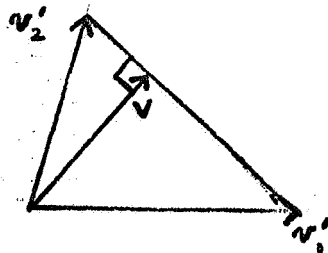


Figure 4 b) calculation of true velocity by construction

We may consider the correlation of amplitude across the observing plane in terms of the correlation between points in that plane. The autocorrelation of amplitude at a point is connected to the cross correlation between points by the velocity of the correlation pattern. This in turn is related to the actual velocity of the phase changing screen. At any instant of time we may compare crosscorrelation between stations to the corresponding value of autocorrelation to obtain a characteristic time delay for this value. Dividing this into the distance between the stations gives us a characteristic velocity for that direction (this is considered in more detail in Internal Report 4). It is these values which have been plotted as Figure 2. We fit an ellipse to these values of characteristic velocity and transform to a coordinate system where this ellipse becomes a circle and proceed to calculate velocity as before. We then transform everything back to the observing plane and we have the true velocity of the medium as projected on the observing plane.

While this procedure is completely straightforward, it is much more prone to error than is the lag analysis alone. With the caution that it does not check assumptions, the lag analysis shows the errors in reduction. The shape analysis uses actual measures of correlation and is thus sensitive to a number of sources of error. We have gone to great lengths to eliminate these errors (See e.g. Report 5) but some, no doubt, remain. It should be possible to get an estimate of error by predicting correlation at various lags. These will give us a check on the validity of the shape analysis which we carried out with zero lag data. Until this work is completed the values calculated cannot be given accurate error bars. Estimates are, however, listed in Table 5 for reference at this



time.

The three station analysis continues in order to get a meaningful error analysis for Table 5. The two station records of 1965-66 are being analyzed to continue the work of Douglas and Smith and will be expanded to check the possible use of morphological studies of the L pulses present in these and the single station records.

TABLE 3

Summary Of Analysis Assuming Circular Contours Of Equal Correlation

Data	Projected Velocity	Angle Between Velocity Vector and Projection of The Ecliptic
23 Oct 65	250 km./sec.	-20°
26 Oct 65	320 km./sec.	-15°
14 Dec 65	360 km./sec.	53°

TABLE 4

Summary of Shape Analysis

Data	Axial Ratio of Correlation Contour	Angle Between Major Axis of Correlation Ellipse and Ecliptic
23 Oct 65	3.7	41°
26 Oct 65	10.2	26°
14 Dec 65	3.7	64°

TABLE 5

Summary of Velocity Analysis After Correcting for Shape

Data	Projected Velocity	Angle Between Velocity Vector and Projection of The Ecliptic
23 Oct 65	400 km./sec.	31°
26 Oct 65	350 km./sec.	19°
14 Dec 65	600 km./sec.	-14°

Errors in velocities tabulated in Table 5 are about  $\pm 40\%$  in magnitude and  $\pm 25^\circ$  in direction (see text).

References

Douglas, J. N. and Smith, H. J. 1967. Ap.J. 148, 885.

Internal Reports Appended To Previous NASA Reports

Report #3. In Final Report NASA grant NsG407 to Yale University,  
20 December 1966.

Report #4. In Semi-annual Status Report NASA grant SC-NGR-44-012-055  
to the University of Texas, May 1966-October 1966.

Perry, J. W. "Study of S Pulse Activity etc." Ibid.

Report #5. In Semi-annual Status Report NASA grant SC-NGR-44-012-055  
the University of Texas, November 1966-May 1967.

## APPENDIX

In the correlation graphs which follow the axes are time in seconds and normalized correlation. The crosscorrelation labels refer to data from two stations, e.g. x,y. In a graph of crosscorrelation x-y a positive delay to peak correlation means a delay in the sense that y lags x. The dash on the graphs means only "and" or "versus". This differs from the terminology of Douglas and Smith (1967) where the dash meant "minus". To compare with their tabulation the labels should be reversed. Then x-y becomes y-x where the dash represents the concept "minus" and a positive delay means y lags x.

The station coordinates are given by Douglas and Smith (1967) the graphs labels are:

B - Bethany, Connecticut

H - in 1961 Hendrie Hall, New Haven, Connecticut  
in 1965 Huntington, New York

M - Middletown, Connecticut

P - Pomfret, Connecticut